water

MDPI

*Article*

# Experimental Investigation of the Evolution Process of Suspended Pipelines through River Bottoms under Unsteady Flow Conditions

**Changjing Fu [1,2], Yangming Xu [1] and Tianlong Zhao [1,*]**

[1] National Engineering Research Center for Inland Waterway Regulation, Chongqing Jiaotong University, Chongqing 400074, China; nhri_fuchangjing@163.com (C.F.); xuyangming316@163.com (Y.X.)
[2] Department of Civil Engineering, Monash University, Clayton, VIC 3800, Australia
* Correspondence: neo_3303@163.com

**Abstract:** One of the major geological hazards that can cause harm to long-distance oil and gas pipelines are water-induced disasters. These disasters are quite common and widespread. Pipelines that cross river channels are at a higher risk of facing damage due to flood-induced erosion. To shed light on the evolution pattern of riverbeds adjacent to pipelines under the influence of unsteady flow conditions, a flume model test was conducted, and the underlying mechanisms of local scour were elucidated. The experimental results demonstrate that pipelines are more susceptible to suspension during flood conditions. The suspension process of pipelines under flood conditions could be broadly divided into five stages. In comparison to constant flow conditions, the evolution process of local scour and the suspension of pipelines under unsteady flow lacked the erosion pit expansion stage, and the scour duration was shorter. Each stage exhibited distinct erosion characteristics, and both the peak flow rate and the number of flood peaks significantly impacted the maximum range and depth of the erosion pit. During pipeline-laying projects, selecting a covering layer with a larger particle size can enhance the erosion resistance of the riverbed around the pipeline. The study of the local erosion process of underwater crossing pipelines under unstable flow conditions can provide a reference for pipeline engineering design and riverbed pipeline protection strategies.

**Keywords:** river crossing pipeline; unsteady flow; erosion test; factor analysis



**Citation:** Fu, C.; Xu, Y.; Zhao, T. Experimental Investigation of the Evolution Process of Suspended Pipelines through River Bottoms under Unsteady Flow Conditions. *Water* **2024**, *16*, 336. https://doi.org/10.3390/w16020336

Academic Editor: Roberto Gaudio

Received: 24 November 2023
Revised: 21 December 2023
Accepted: 8 January 2024
Published: 19 January 2024



## 1. Introduction

As China's economy and population continue to grow rapidly, the demand for oil and gas is increasing at an accelerated rate. To meet this demand, long-distance oil and gas pipelines are being constructed. In the southwestern region of China, where there are many rivers and dense networks of waterways, these pipelines will need to cross some of these waterways, posing safety issues during their construction and operation.

According to literature statistics [1], over 90% of under-river pipeline crossings in oil transportation projects are buried in trenches. With the continuous increase in service life, the covering layer of some pipes gradually thins under the action of water flow erosion. Especially during flood periods, deteriorated water flow conditions significantly increase the probability of instability and damage to river crossing pipelines. Based on on-site investigations and data analysis of hundreds of damaged pipelines in central and western China [2], flood-related pipeline damage was found to account for 59% of the cases. Furthermore, unsteady flow, in which the quantity of liquid flowing per second is not constant, is formed due to variations in flow rate and water level over time during flood discharge. Therefore, the impact of unsteady flow erosion on the safe operation of long-distance pipelines cannot be overlooked [3].

Currently, experimental research on the local erosion of pipelines primarily focuses on flow (steady flow), waves, and wave-flow interactions. Many studies have established

empirical formulas for maximum scour depth through model tests and analyzed the influencing factors of scour depth [4,5]. Postacchini et al. [6] examined the erosion process around pipelines in weakly cohesive seabed soil under the influence of waves and currents, with test results indicating that scouring depth was related to seabed soil properties. Gao et al. [7] studied the relationship between pipeline vibration and bed scours using test methods. Zhao et al. [8] conducted experimental research on the local scour of pipelines under constant flow conditions, detailing the effects of factors such as pipe diameter and flow velocity on maximum erosion depth. Cheng et al. [9] investigated the local scour of pipelines on slopes under regular wave action, finding that the depth and width of erosion exhibit two stages with time. Subsequently, relevant scholars discussed local scour time around pipelines in different seabed soils, analyzing relevant influencing factors [10,11]. Sumer et al. [12] studied the erosion process of circular structures in three types of seabed soil under wave action through experimental methods, finding that the sandy soil layer had the shortest erosion time. Dogan et al. [13] analyzed the impacts of varying pipeline diameters, sediment particle sizes, and wave parameters on the time required for sediment erosion to reach equilibrium. Hairsine et al. [14] presented a new method for predicting sediment sorting associated with soil erosion for non-equilibrium conditions. Pontillo et al. [15] studied the validation of a one-dimensional numerical code applied to an unsteady two-phase flow over an initially trapezoidal-shaped sediment dike, including the transition from sub- to supercritical flows and the flow propagation over a steep slope. Hong et al. [16] explored the maximum scour depths and their locations for two different riprap apron lengths downstream of the spillway stilling basin; these were measured along with the complex flow fields prior to scour. Evangelista et al. [17] presented some laboratory experimental results of erosion of a sand dike produced by the impact of a dam break wave.

With the continuous increase of service life, the covering layer of some pipes gradually thins under the action of water erosion, leading to local suspended instability and risks such as pipeline burst and leakage. Consequently, excessive deflection (excessive undermining) results in suspended pipe failure [18,19]. Once accidents such as pipeline explosions or leaks occur, they severely affect public safety, endanger the ecological environment, and cause significant economic losses and social impacts. In recent years, many scholars have started paying attention to the local erosion and suspension process of pipelines and their instability mechanisms. Yang et al. [20] conducted a model test on underwater crossing pipelines, studying the mechanism of local erosion in pipelines. Wu et al. [21] presented experimental research results on the mechanism of lateral erosion propagation in pipelines. Zhao et al. [22] investigated the local erosion mechanism of submarine pipelines. Liu [23] predicted local erosion around submarine pipelines under wave action in shallow water. Matteo et al. [6] studied the erosion process around submarine pipelines in weakly viscous seabed. Ahmad et al. [24] found that the erosion phenomenon below pipelines was essentially a random process.

Regarding sediment transport under different water flow conditions, many research works have been conducted. Macvicar et al. [25] used Radio Frequency Identification (RFID) transponders to compare the short-term (1 year) sediment transport response to flood events in a restored and a control reach. Williams et al. [26] assessed a depth-averaged nonuniform sediment model (Delft3D) to predict the morphodynamics of a 2.5 km long reach of the braided Rees River, New Zealand, during a single high-flow event. Dysarz et al. [27] tested forecasting of the sediment transport process, considering two main uncertainties involved in sediment transport modeling. Eshev et al. [28] discussed the problems of determining the friction parameter and non-eroding conditions in a wave flow, considering them from the standpoint of an approach using a critical dynamic speed. Zhao et al. [29] conducted flume scour tests regarding the discharge process of the barrier dam, and studied the scouring characteristics of wide-graded sediment under different flow conditions.

Many researchers have conducted extensive studies on the process and factors leading to the erosion of underwater pipelines in various locations. However, most of these studies have focused on pipelines located in the ocean, considering the impact of waves or the

combined effect of constant currents and waves. Currently, there are few experimental studies on the erosion of pipeline crossings at the bottom of rivers under the influence of unsteady flow forces. In this research, a series of flume model experiments were conducted to investigate the suspended evolution process of river crossing pipelines under unsteady flow. The influencing factors of local erosion and suspension, such as flood, pipeline, and bed sand, were analyzed, and based on this, the evolution mechanism of suspended pipelines under unsteady flow conditions was analyzed.

## 2. Laboratory Experiment

### *2.1. Experimental Facility*

The experiment was conducted in the high-precision and multifunctional variable slope experimental flume system of the National Inland Waterway Regulation Engineering Technology Research Center of China. The experimental water tank system comprised a glass tank, a sedimentation tank, a clear water reservoir, a water pump, a tailgate, a valve, and a return pipe. A water supply and backwater system utilizing frequency conversion technology was installed in the water tank system, enabling the generation of arbitrary shapes and continuous unsteady water flow.

The test flume of the channel was 28 m long, 0.56 m wide and 0.8 m high. The test tank had a fully transparent and high-strength glass trough structure. The boundary of the tank could be adjusted, and the overall accuracy could reach ±0.2 mm. The diagram of the sink is shown in Figure 1.

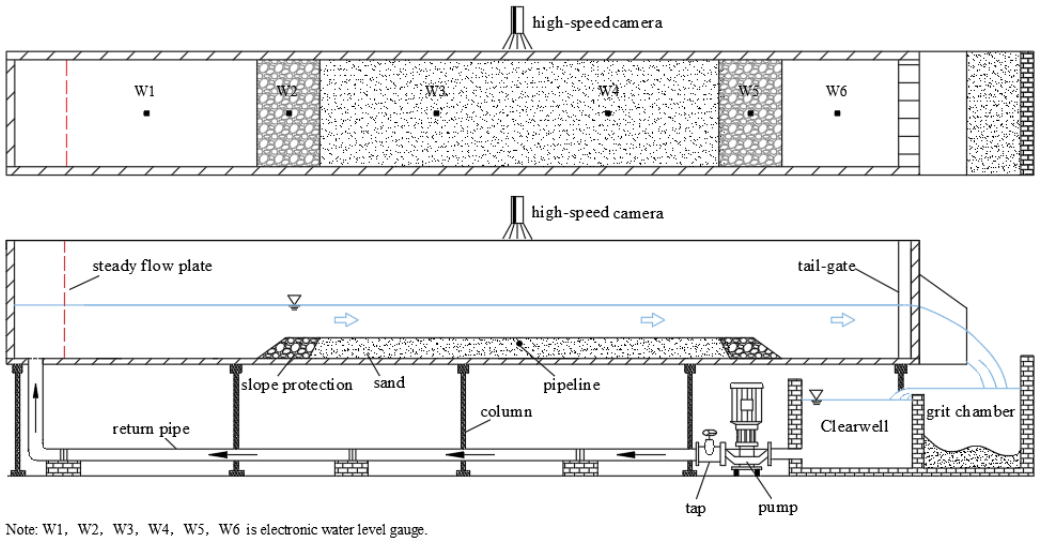


**Figure 1.** The schematic diagram of the flume test model.

### *2.2. Experimental Scale*

As inertia force and gravity are the dominant factors in the process of river scour, the gravity similarity criterion (also known as the Froude similarity criterion) was adopted. The experiment was designed as a normal model, with the model scale detailed in Table 1.

**Table 1.** The scale of the model test.

| Parameter | Similar Scale Relationship | Similarity Ratio |
|---|---|---|
| Geometric length $l$ (m) | $\lambda_L$ | 40 |
| The velocity of flow $v$ (m/s) | $\lambda_v = \lambda_L^{0.5}$ | 6.32 |
| Time $t$ (s) | $\lambda_t = \lambda_L^{0.5}$ | 6.32 |
| Water flow rate $Q$ ($m^3$/s) | $\lambda_Q = \lambda_L^{2.5}$ | 10,119.3 |
| Pressure $P$ (Pa) | $\lambda_P = \lambda_L$ | 40 |

The test water temperature was maintained at 20 °C. The Froude number was calculated. The results are shown in Table 2. It can be seen, from Table 2, that the Froude number before the flood peak was between 0.417 and 0.817, both of which were smaller than the critical flow $Fr = 1$. It indicated that the water flow before the flood peak was tranquil. After reaching the flood peak, the calculated Froude number at the flood peak was between 1.129 and 1.449, both of which were greater than the critical flow $Fr = 1$. It indicated that the water flow at the flood peak was rapid.

**Table 2.** The Froude number of the model test.

| Working Condition | Maximum Peak Discharge (L/s) | The Average Flow Velocity (m/s) | The Cross-Sectional Area ($cm^2$) | Width of Channel (cm) | Downstream Water Depth (cm) | *Fr* |
|---|---|---|---|---|---|---|
| Pre-flood peak | 12.8 | 0.44 | 162.4 | 56 | 2.9 | 0.817 |
| | 11.7 | 0.36 | 207.2 | 56 | 3.7 | 0.592 |
| | 10.8 | 0.28 | 252 | 56 | 4.5 | 0.417 |
| Reached flood peak | 12.8 | 0.86 | 196 | 56 | 3.5 | 1.449 |
| | 11.7 | 0.78 | 224 | 56 | 4.0 | 1.216 |
| | 10.8 | 0.73 | 235.2 | 56 | 4.2 | 1.129 |

### 2.3. Experimental Scheme

The test section was positioned at the center of the water tank, with a length of 1.2 m and a height of 0.08 m. The slope protection, laid before and after the experimental section, consisted of gravel with a particle size exceeding 1 cm. The layout of the test section is displayed in Figure 2.

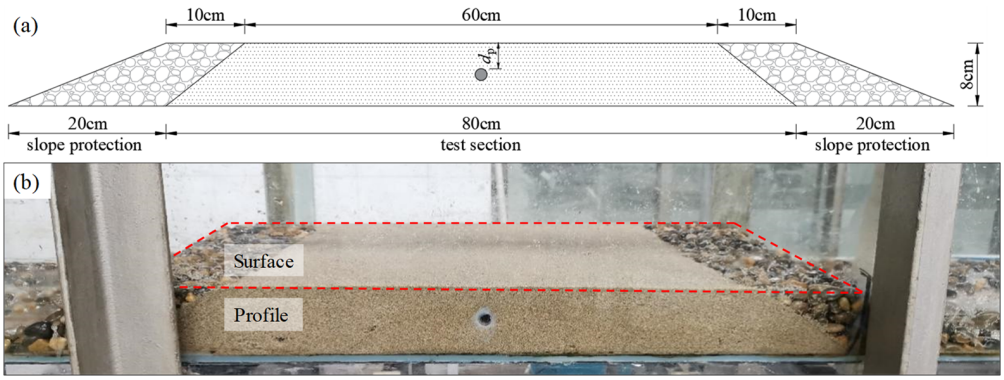


**Figure 2.** Layout diagram of the test section. (**a**) Schematic diagram of the cross-section of the test section. (**b**) Image of the test section.

For this test, standard quartz sand was selected. Referring to national standards, fine sand measures $d_{50}$ = 0.25–0.10 mm, medium sand $d_{50}$ = 0.5–0.25 mm, and coarse sand $d_{50}$ = 1–0.5 mm. In this test, the fine sand measured $d_{50}$ = 0.125 mm, the medium sand $d_{50}$ = 0.55 mm, and the coarse sand $d_{50}$ = 0.95 mm (as illustrated in Figure 3). Regarding the fine and medium sand, sand waves tended to form on the surface of the experimental erosion section. These waves may have affected the development of erosion pits to some extent, and even the suspension process of pipelines. However, this research primarily focused on the scouring process of sand in the lower part of the riverbed-buried pipeline under unsteady flow. The experiments revealed that sand waves are relatively small and have a weak scouring effect on sediment. Therefore, this study ignored the influence of sand wave development on the scouring process.

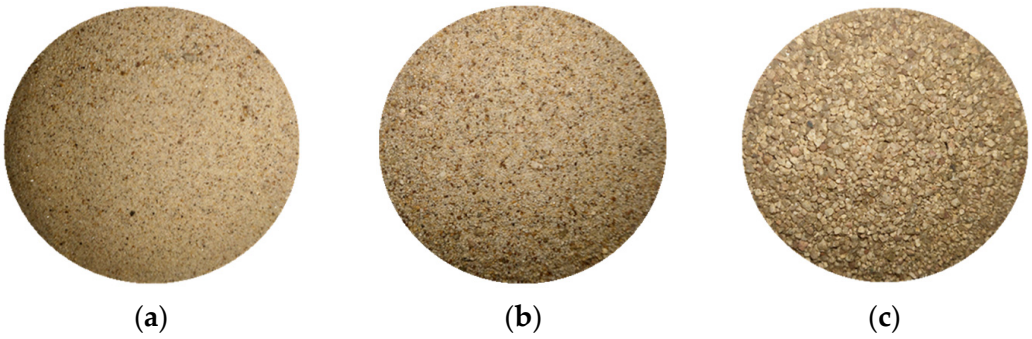


**Figure 3.** Model sands used for testing. (**a**) Fine sand ($d_{50}$ = 0.125 mm). (**b**) Medium sand ($d_{50}$ = 0.55 mm). (**c**) Coarse sand ($d_{50}$ = 0.95 mm).

Based on the riverbed particle results from investigations conducted on several rivers in southwestern China, the design was carried out with a length scale ratio $\lambda_L$ = 40, and the grading curve of the model sands is shown in Figure 4.

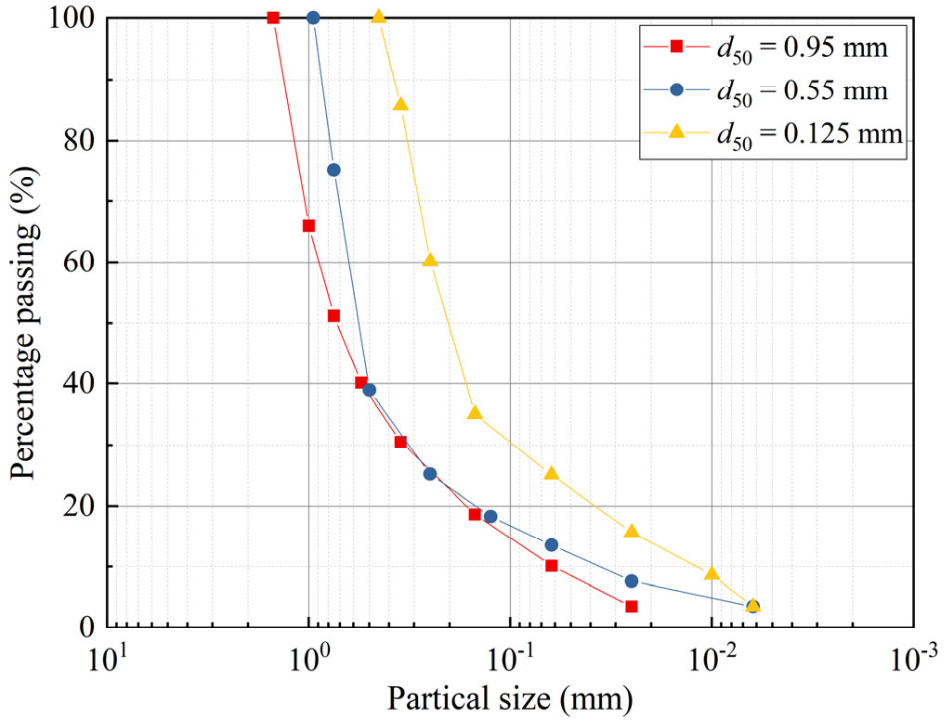


**Figure 4.** Model sands grading curve.

A hollow, smooth PVC pipe with a diameter of 1.5 cm was utilized as the experimental pipeline. Positioned in the center of the test section, the pipeline was designed to mimic the construction of a river crossing pipeline. To minimize the river crossing length, it is typical for the pipeline to maintain a 90° angle relative to the flow direction. However, adjustments to the laying angle may be necessary, requiring the angle to be maintained between 60° and 90°. In this test, the pipeline's axis and water flow direction were analyzed at 60° and 90° angles, respectively, to examine the scouring process. The layout of the pipeline angles is illustrated in Figure 5.

In this research, the analysis of sediment erosion process and influencing factors was based on image processing of sediment erosion process. To obtain reliable erosion data, such as erosion depth and range, from the images, the author used a horizontal ruler to ensure that the camera lens was facing vertically towards the glass on the side of the flume before the

experiment. After the experiment, the authors washed the residual test sand with clean water and used a sand funnel downstream to ensure that all residual test sand was collected.

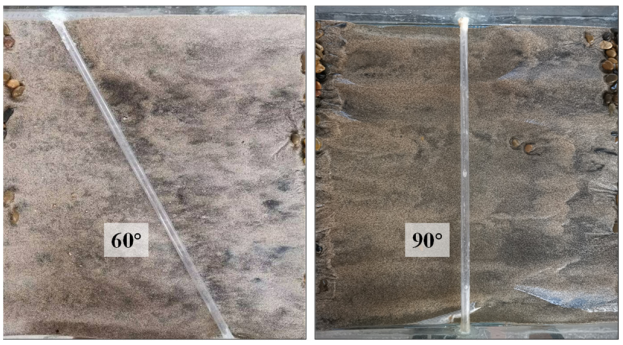


**Figure 5.** The angle arrangements of pipeline laying.

### *2.4. Experimental Conditions*

The evolution of a riverbed around underwater crossing pipelines is influenced by various factors, such as water flow conditions, bed sediment characteristics, pipeline size, burial depth, etc. This paper investigated the influence of these factors and the physical erosion processes caused by unsteady flow on the local erosion of the riverbed around river crossing pipelines.

To account for the varying river water flows in southwestern China, it was crucial to consider how different flow conditions affect the local erosion of river bottom crossing pipelines. For the test, the flood hydrograph data [30] from three regions in southwestern China were used (as depicted in Figure 6). In these three flood hydrographs, the peak and base flow used by the authors in their experiments were based on the data from Shuangfu Hydrological Station (Caijia river and Damakou hydrological station did not have base flow results, and their peak flow values were small. The scaled test flow peak values according to the experimental setting scale could not cause the initiation and erosion of sand in the test section). The waveform used in the experiment mainly refers to the Damakou hydrological station, and the flood waveform used in the experiment was obtained through scaling. The specific test conditions are shown in Table 3.

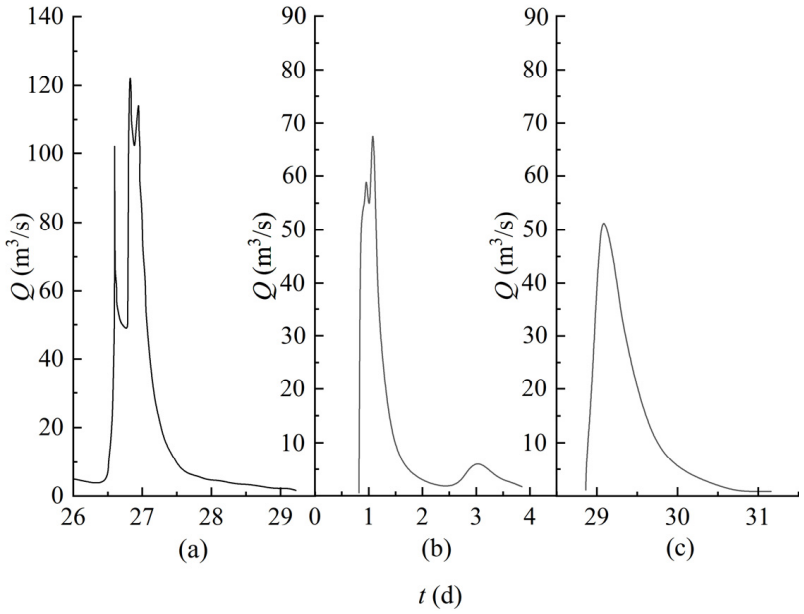


**Figure 6.** Flood hydrographs of rivers in southwestern mountainous areas (monitored by different hydrological stations). (**a**) Shuangfu. (**b**) Caijia river. (**c**) Damakou.

**Table 3.** Test conditions.

| Test Condition Group | Pipe Diameter $d$ (cm) | Maximum Peak Discharge $Q_p$ (L/s) | Type of Flood | Particle Size of Sand $d_{50}$ (mm) | Laying Angle $\theta$ | Relative Density $D_r$ (g/cm$^3$) | Burial Depth $d_p$ (cm) |
|---|---|---|---|---|---|---|---|
| I | 1<br>1.5<br>2 | 12.8 | Unimodal flood | 0.55 | 90° | 1.24 | 3 |
| II | 1.5 | 12.8<br>11.7<br>10.8 | Unimodal flood | 0.55 | 90° | 1.24 | 3 |
| III | 1.5 | 12.8 | Unimodal flood<br>Bimodal flood<br>Triple peak flood | 0.55 | 90° | 1.24 | 3 |
| IV | 1.5 | 12.8 | Unimodal flood | 0.125<br>0.55<br>0.95 | 90° | 1.24 | 3 |
| V | 1.5 | 12.8 | Unimodal flood | 0.55 | 60°<br>90° | 1.24 | 3 |
| VI | 1.5 | 12.8 | Unimodal flood | 0.55 | 90° | 1.24<br>1.32<br>1.40 | 3 |
| VII | 2 | 12.8 | Unimodal flood | 0.55 | 90° | 1.24 | 3<br>4 |

It should be noted that this study focused on the impact of riverbed erosion on the stability of structures under flood conditions. Water flow under flood conditions often has strong unsteady characteristics, and the riverbed often has higher roughness than the seabed, resulting in strong turbulence in the near-bottom flow. In this case, the mainstream may dominate the erosion process of the bed sediment. Therefore, in this study, to simplify the problem, authors ignored the impact of secondary flow generated by rough pebbles in the slope protection section on erosion.

## 3. Experimental Results and Discussions

### *3.1. The Suspended Evolution Process of River Crossing Pipelines under Unsteady Flow*

Owing to the randomness and variability of sand particle initiation under the influence of unsteady flow, qualitative analysis of the erosion process of the river crossing pipeline could only be performed through physical observation. During the process of examining the local erosion images captured by the camera, the experimental observation window played a vital role. This window was positioned near the pipeline and measured 60 cm × 10 cm. It was discovered that the progression of riverbed erosion occurred in five distinct stages, which have been illustrated in Figure 7 based on the images captured by the camera.

Stage 1: Riverbed cutting. Under the erosion of flow, sand particles are transported downstream with the current. Due to the lack of upstream sand supply, the riverbed continues to cut down and the burial depth of the pipeline gradually decreases.

Stage 2: Pipeline exposure. During riverbed cutting, the presence of the pipeline alters the flow field around it, leading to accelerated cutting of the riverbed until the pipeline is exposed. Due to the formation of vortices near the pipeline caused by the water flow, local scour holes appear downstream of the pipeline under prolonged erosion.

Stage 3: Micro-pore formation. After the pipeline is exposed to the water surface, the local vortex formed in the upstream area of the pipeline transports sand towards the upstream, resulting in local uplift. Meanwhile, the local vortices formed downstream of the pipeline continue to transport sand downstream, causing the local scour pit in the

downstream area to gradually increase. The sand around the pipeline migrates away from the pipeline, eventually leading to the formation of a micro-pore at the bottom of the pipeline.

Stage 4: Pipeline suspended. The water flows through the micro-pore at the bottom of the pipeline, altering the flow field around the pipe and creating a flow past the circular cylinder. This increases the flow velocity at the bottom of the pipeline and accelerates the migration of sand particles. The micro-pore diffuses downwards and develops along the direction of the pipe axis, gradually forming a scouring pit.

Stage 5: Scour balance. Following a prolonged scouring process, the eddy current formed near the pipeline results in a symmetrical erosion profile of the riverbed at the bottom of the pipeline. The scour depth at the bottom of the pipeline remains consistent, indicating the attainment of a scour equilibrium state.

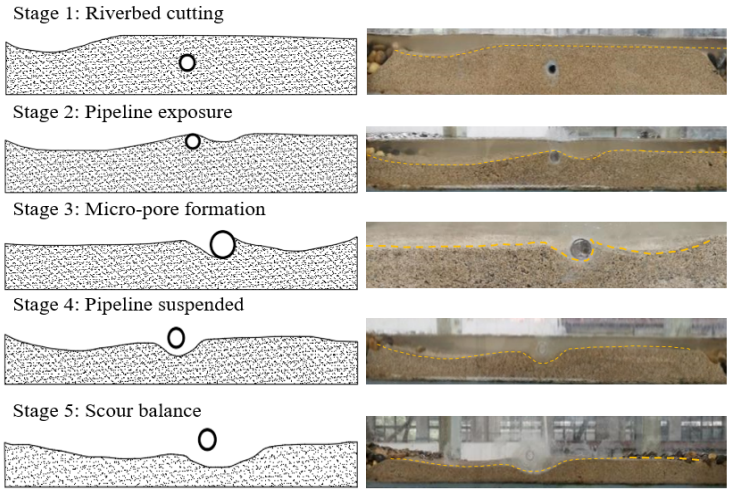


**Figure 7.** The evolution process of riverbed erosion around a river crossing pipeline.

### *3.2. The Influence of Different Flood Parameters*

To examine the impact of varying peak flows on the local erosion of pipelines under unsteady flow conditions, pertinent experimental studies were conducted. The test utilized a unimodal flood type with maximum peak discharges of 10.8 L/s, 12.8 L/s, and 11.7 L/s. The pipeline had a diameter of 1.5 cm, a burial depth of 3 cm, and a laying angle of 90°. The sand used had a particle size of $d_{50}$ = 0.55 mm and a relative density of 1.24 g/cm$^3$. The resulting riverbed erosion patterns around the pipeline under different peak discharges are illustrated in Figure 8.

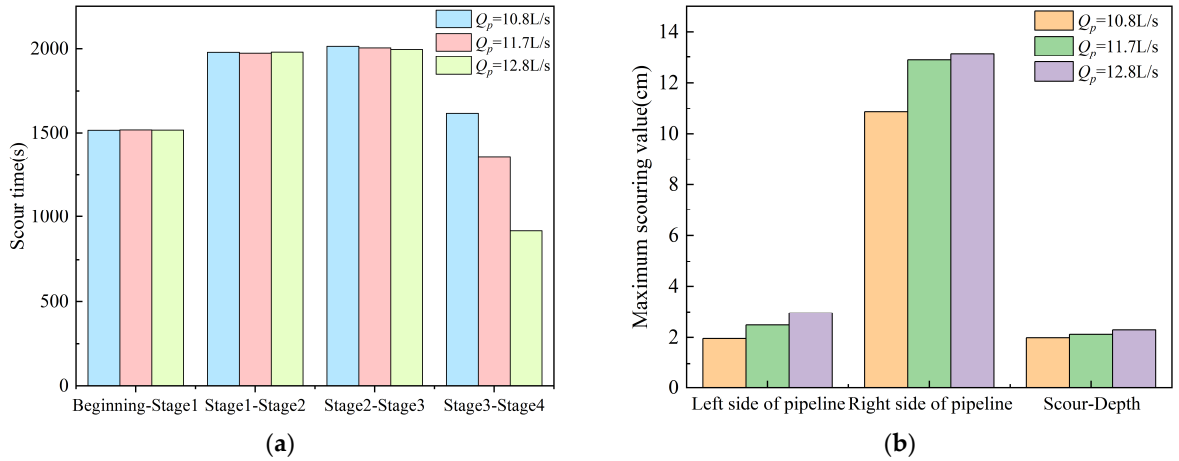


**Figure 8.** The situation of riverbed erosion around the pipeline under different peak discharges. (**a**) Scour time. (**b**) Maximal scour depth.

The experiment revealed that the degree and speed of riverbed cutting remained consistent before the arrival of the flood peak, with the exposure time of pipeline parts being roughly equivalent to the formation speed of the micro-pore. However, under varying flood peak values, the time taken for the micro-pore at the bottom of the pipeline to form and the pipeline to become fully suspended decreased when the maximum flood peak value increased. As the maximum flood peak increased, the maximum erosion depth near the pipeline became greater and the maximum erosion range widened after achieving erosion equilibrium. From Figure 8, it can be seen that the peak flow rate increased by 18.5%, resulting in a 15% increase in erosion depth.

To explore the impact of various flood types on the local erosion of pipelines under unsteady flow conditions, pertinent experimental studies were conducted. The experiment incorporated three flood types: unimodal flood, bimodal flood, and triple peak flood, with a maximum peak discharge of 12.8 L/s. The pipeline had a diameter of 1.5 cm, a burial depth of 3 cm, and a laying angle of 90°. The sand used had a particle size of $d_{50}$ = 0.55 mm and a relative density of 1.24 g/cm$^3$. The resulting riverbed erosion patterns around the pipeline under different flood types are presented in Figure 9.

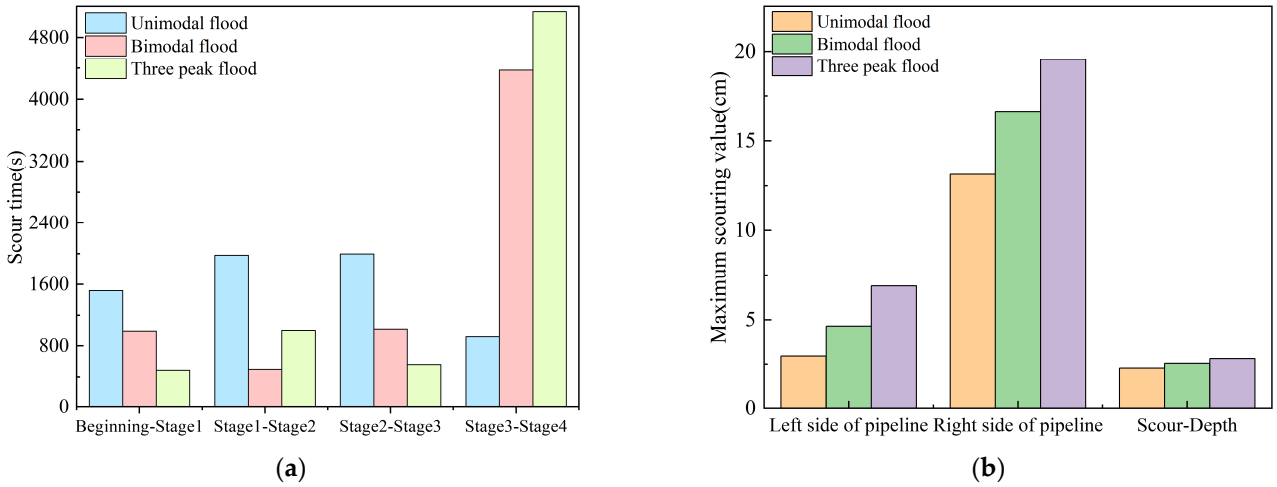


**Figure 9.** The situation of riverbed erosion around the pipeline under different flood types. (**a**) Scour time. (**b**) Maximal scour depth.

The experiment revealed that, under the same total scouring time, the degree and speed of riverbed undercutting underwent significant changes when compared to a single unimodal flood. Additionally, the exposure time of pipeline parts and the formation speed of micro-pores increased notably under the conditions of bimodal and triple peak floods. As the number of flood peaks increased, the riverbed-cutting process became shorter, and the time taken from micro-pore formation to complete suspension of the pipeline was reduced. Consequently, the maximum scour depth near the pipeline became greater, and the maximum erosion range widened after achieving erosion equilibrium.

### *3.3. The Influence of Different Pipeline Parameters*

To examine the impact of varying pipe diameters on the local erosion of pipelines under unsteady flow conditions, pertinent experimental studies were conducted. The experiment utilized a unimodal flood type with a maximum peak discharge of 12.8 L/s. Three pipe diameters were tested: 1.0 cm, 1.5 cm, and 2.0 cm, with a burial depth of 3 cm and a laying angle of 90°. The sand used had a particle size of $d_{50}$ = 0.55 mm and a relative density of 1.24 g/cm$^3$. The resulting riverbed erosion patterns around the pipeline under different pipe diameters are presented in Figure 10.

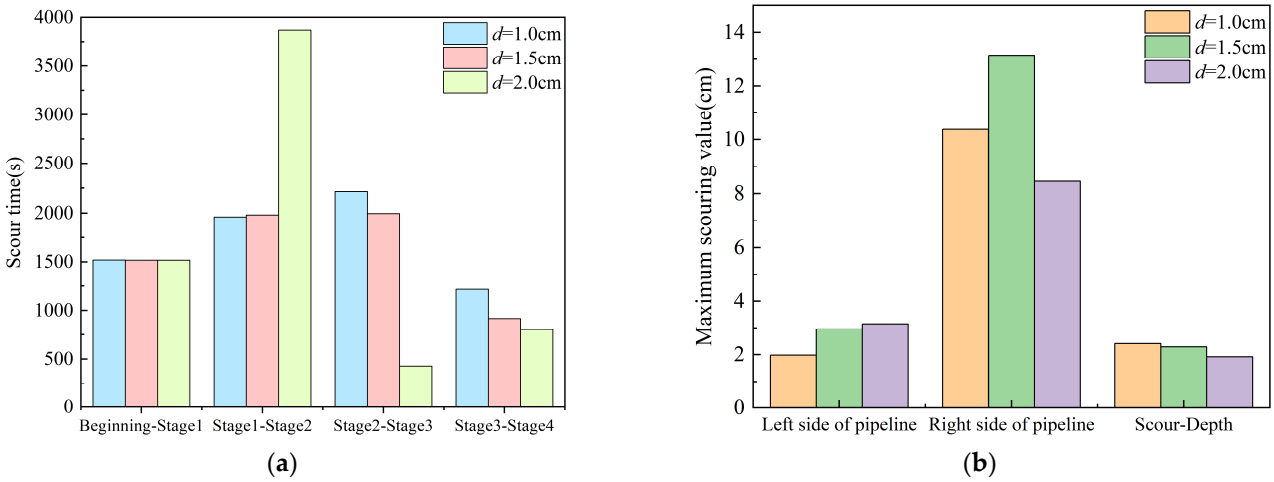


**Figure 10.** The situation of riverbed erosion around the pipeline under different pipe diameters. (**a**) Scour time. (**b**) Maximal scour depth.

The experiment demonstrated that the velocity of riverbed cutting remained steady, yet the exposure duration lengthened as the pipeline diameter increased. When the pipeline was exposed, a larger diameter resulted in a reduced time frame for the pipeline to become fully suspended. Through careful observation and measurement of the scouring pits surrounding the pipeline after erosion equilibrium was attained, it was discovered that the maximum scouring depth near the 1.5 cm diameter pipeline was greater, with a wider maximum scouring range. However, overall, by observing and measuring the erosion pits around the pipeline after reaching erosion equilibrium, the experiment indicated that as the diameter of the pipeline decreased, the range of the erosion pits became larger, and the maximum depth of erosion became deeper. From Figure 10, it is also indicated that when the diameter of pipeline increased by 100%, there was a 25.5% increase in erosion depth.

To investigate the influence of different pipe-laying angles on the local erosion of pipelines under unsteady flow, relevant experimental studies were conducted. In this experiment, a unimodal flood type with a peak flow of 12.8 L/s was adopted. The diameter of the pipe was 1.5 cm, the burial depth was 3 cm, and the laying angles were 60° and 90°. The particle size of the sand used was $d_{50}$ = 0.55 mm, the relative density was 1.24 g/cm$^3$. The situation of riverbed erosion around the pipeline under different pipe-laying angles is shown in Figure 11.

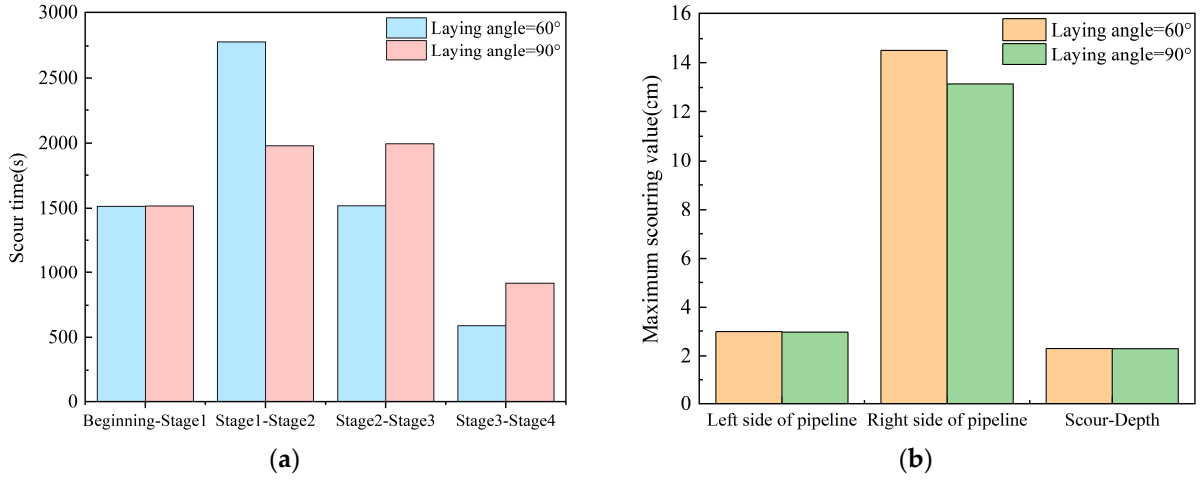


**Figure 11.** The situation of riverbed erosion around the pipeline under different pipe-laying angles. (**a**) Scour time. (**b**) Maximal scour depth.

It was discovered that, at the pipeline-laying angle of 60°, the time taken for pipeline exposure was notably extended. For varying pipeline-laying angles, following the attainment of scouring equilibrium, the scouring extent of the bed around the pipeline (specifically, on the right side of the pipeline, or in the downstream direction) exhibited slight differences, while the maximum scouring depth remained consistent.

To explore the impact of varying pipe-burial depths on the local erosion of pipelines under unsteady flow conditions, pertinent experimental studies were conducted. In this experiment, a unimodal flood type with a maximum peak discharge of 12.8 L/s was adopted. The pipe had a diameter of 1.5 cm and was buried at depths of 3 cm and 4 cm, respectively, with a laying angle of 90°. The sand used had a particle size of $d_{50}$ = 0.55 mm and a relative density of 1.24 g/cm$^3$. The resulting riverbed erosion patterns around the pipeline under different pipe-burial depths are presented in Figure 12.

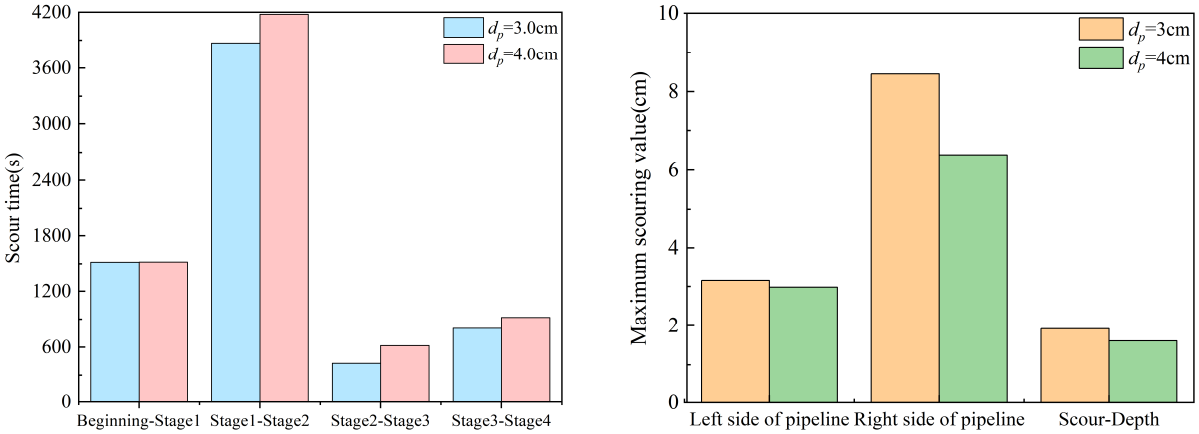


**Figure 12.** The situation of riverbed erosion around the pipeline under different burial depths. (**a**) Scour time. (**b**) Maximal scour depth.

The test indicated that, with the increase in the burial depth of the pipeline, the time taken for local erosion of the pipeline to occur in suspension noticeably lengthened. As the burial depth of the pipeline augmented, the maximum erosion range contracted, and the maximum erosion depth became less profound. This suggests that enhancing the burial depth can improve the safety of pipeline operations. From Figure 12, it is revealed that when the burial depths increased by 30%, erosion depth decreased by 13.6–16% decrease in erosion depth.

### *3.4. The Influence of Different Bed Sand Parameters*

To examine the impact of varying bed-relative densities on the local erosion of pipelines under unsteady flow conditions, pertinent experimental studies were conducted. The experiment utilized a unimodal flood type with a maximum peak discharge of 12.8 L/s. The pipe diameter was 1.5 cm, the burial depth was 3 cm, and the laying angle was 90°. Three relative densities of sand were tested: 1.24 g/cm$^3$, 1.32 g/cm$^3$, and 1.40 g/cm$^3$. The relative density values were obtained through a combination of experimental measurements and theoretical calculations, with relative density defined as (soil volume density/maximum dry density) × 100%. Soil volume density was determined by dividing the total mass of laid test sand by the volume of the test section, while the maximum dry density was acquired from indoor geotechnical tests.

The situation of riverbed erosion around the pipeline under different bed-relative densities is shown in Figure 13. From this, it was found that when the relative density increased by 12.9%, erosion depth decreased by 6%.

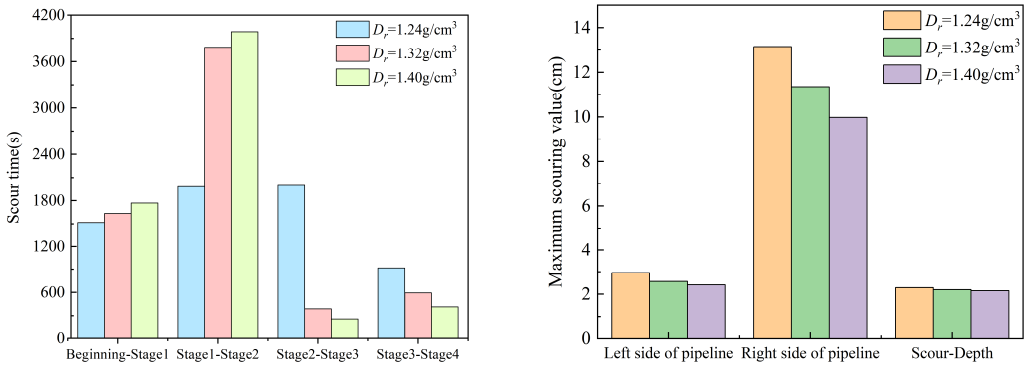


**Figure 13.** The situation of riverbed erosion around the pipeline under different bed-relative densities. (**a**) Scour time. (**b**) Maximal scour depth.

It was discovered that the erosion duration from the initiation to the pipeline exposure stage was significantly longer for relative densities of 1.32 g/cm$^3$ and 1.40 g/cm$^3$ in comparison to the test condition with a density of 1.24 g/cm$^3$. As the bed sand density increased, both the range of scouring pits and the maximum scour depth around the pipeline decreased.

To investigate the influence of different particle sizes of sand on the local erosion of pipelines under unsteady flow, relevant experimental studies were conducted. The experiment adopted a unimodal flood type, and the maximum peak discharge was 12.8 L/s. The diameter of the pipe was 1.5 cm, the burial depth was 3 cm, and the laying angle was 90°. The particle sizes of the sand were $d_{50}$ = 0.125 mm, $d_{50}$ = 0.55 mm, and $d_{50}$ = 0.95 mm; the relative density was 1.24 g/cm$^3$. The situation of riverbed erosion around the pipeline under different particle sizes of sand is shown in Figure 14.

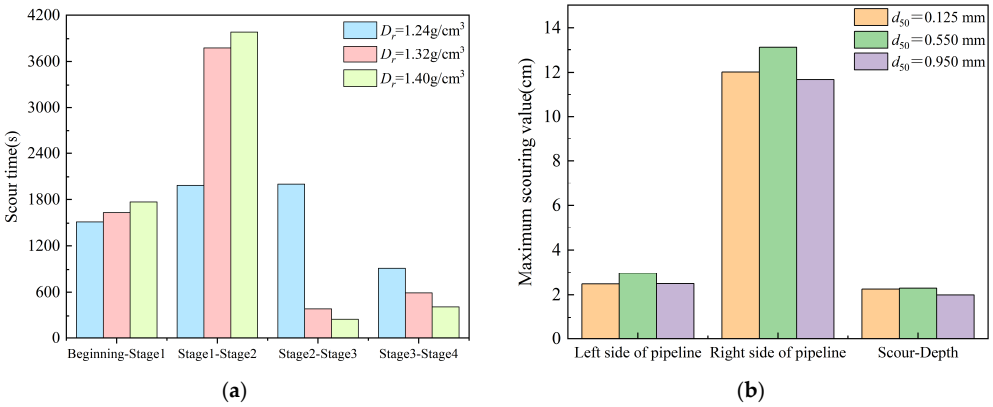


**Figure 14.** The situation of riverbed erosion around the pipeline under different particle sizes of sand. (**a**) Scour time. (**b**) Maximal scour depth.

The results indicated that the duration from the initiation stage to riverbed cutting with a sand particle size of $d_{50}$ = 0.95 mm was much longer than for the others. However, the erosion duration during the stage of pipeline exposure to the micro-pore formation was extremely short. Moreover, the range and maximal scour depth of the scour pit significantly decreased with the increase in particle size.

The results demonstrated that the duration from the initial stage to riverbed cutting was considerably longer when using sand with a particle size of $d_{50}$ = 0.95 mm compared to other sizes. However, the erosion duration during the pipeline exposure to micro-pore formation was exceedingly brief. Furthermore, as the particle size increased, both the range and maximum scour depth of the scour pit notably decreased.

### *3.5. Sensitivity Analysis*

When the depth and range of riverbed erosion around the pipeline no longer change under the action of flow erosion, it can be considered that the erosion of the bed sand around the pipeline has reached a scour equilibrium state. Then, the range of the scour pit and the maximum scour depth of bed sand around the pipeline were recorded. By comparing the results, the maximum scouring difference for each test condition was obtained, as presented in Table 4.

**Table 4.** Maximum scouring difference under different test conditions.

| Maximum Scouring Difference | Influence Factors | | | | | | |
|---|---|---|---|---|---|---|---|
| | **Maximum Peak Discharge** | **Type of Flood** | **Pipe Diameter** | **Laying Angle** | **Burial Depth** | **Relative Density** | **Particle Size of Sand** |
| The left side of the pipeline | 1.00 cm | 3.93 cm | 1.17 cm | 0.03 cm | 0.14 cm | 0.55 cm | 0.48 cm |
| The right side of the pipeline | 2.29 cm | 6.38 cm | 1.93 cm | 1.38 cm | 2.96 cm | 3.17 cm | 1.46 cm |
| Maximal scour depth | 0.30 cm | 0.53 cm | 0.49 cm | 0.03 cm | 0.38 cm | 0.14 cm | 0.26 cm |

The maximum erosion difference is illustrated in Figure 15. From Figure 15, it can be observed that the order of influence intensity on the maximum scouring range on the left side of the pipeline was as follows: Type of flood > Pipe diameter > Maximum peak discharge > Relative density > Particle size of sand > Burial depth > Laying angle. On the right side of the pipeline, the order of influence intensity on the maximum scouring range was as follows: Type of flood > Relative density > Burial depth > Maximum peak discharge > Pipe diameter > Particle size of sand > Laying angle. In terms of the maximum scouring depth, the order of influence intensity was as follows: Type of flood > Pipe diameter > Burial depth > Maximum peak discharge > Particle size of sand > Relative density > Laying angle. In Table 4, there is a significant difference among burial depths. The main reason for this difference is that when the pipeline begins to be exposed, the slope of the bed on the backwater side of the pipeline is usually greater than that on the upstream side. Therefore, the resistance of the water flow on the backwater side is smaller, and the water flow generates greater kinetic energy during the forward process, making it easier to erode the riverbed. Therefore, during the experiment, the absolute value of the scouring depth on the right side of the pipeline was relatively large. Under different pipeline burial depths, the data oscillated significantly, reflecting a significant difference.

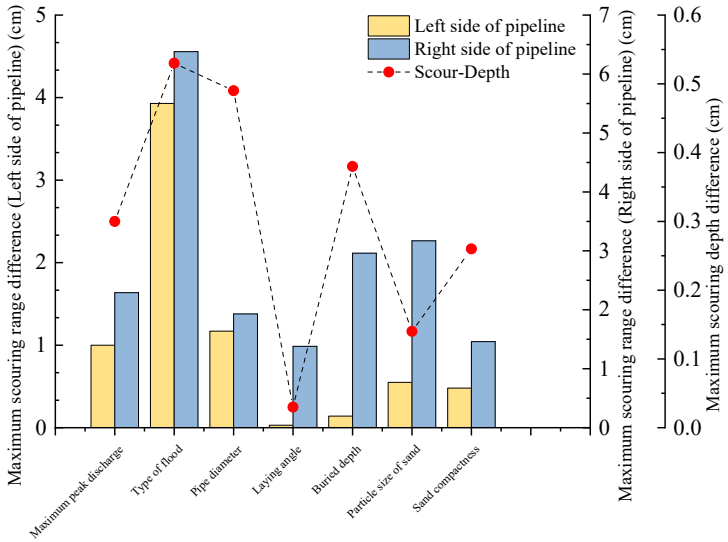


**Figure 15.** The diagram of maximum scouring range and depth difference.

The entire physical scouring process and scouring duration of each stage under different test conditions were recorded, and the maximum scouring duration difference of each scouring stage under each test condition was obtained, as shown in Table 5.

**Table 5.** The maximum difference in scour time under different test conditions.

| Scouring Stage | Maximum Peak Discharge | Type of Flood | Pipe Diameter | Laying Angle | Burial Depth (Increase) | Relative Density | Particle Size of Sand |
|---|---|---|---|---|---|---|---|
| Beginning–Riverbed cutting | 1.91 s | 1031.2 s | 1.84 s | 3.82 s | 2.97 s | 251.66 s | 4006.31 s |
| Riverbed cutting–Pipeline exposure | 6.51 s | 1482.66 s | 1910.51 s | 868.69 s | 21.53 s | 2004.52 s | 1873.84 s |
| Pipeline exposure–Micro-pore formation | 18.3 s | 1423.66 s | 1789.57 s | 502.1 s | 428.4 s | 1749.73 s | 2603.99 s |
| Micro-pore formation–Pipeline suspended | 697.58 s | 4214.59 s | 413.16 s | 349.98 s | 60.41 s | 502.82 s | 624.88 s |

Based on Table 5, the maximum difference in scour time is illustrated in Figure 16. From Figure 16, it can be observed that from the beginning of the experiment to the stage of riverbed cutting, the order of the influence intensity of each factor is as follows: Particle size of sand > Type of flood > Relative density > Laying angle > Burial depth > Maximum peak discharge > Pipe diameter. During the period from riverbed cutting to pipeline exposure, the order of factors affecting the strength of the riverbed was as follows: Relative density > Pipe diameter > Particle size of sand > Type of flood > Laying angle > Burial depth > Maximum peak discharge. In terms of the erosion process from pipeline exposure to micro-pore formation, the order of factors affecting the strength of the pipeline was as follows: Particle size of sand > Pipe diameter > Relative density > Type of flood > Laying angle > Burial depth > Maximum peak discharge. Finally, the intensity of factors affecting the stage from micro-pore formation to pipeline suspension was as follows: Type of flood > Maximum peak discharge > Particle size of sand > Relative density > Pipe diameter > Laying angle > Burial depth.

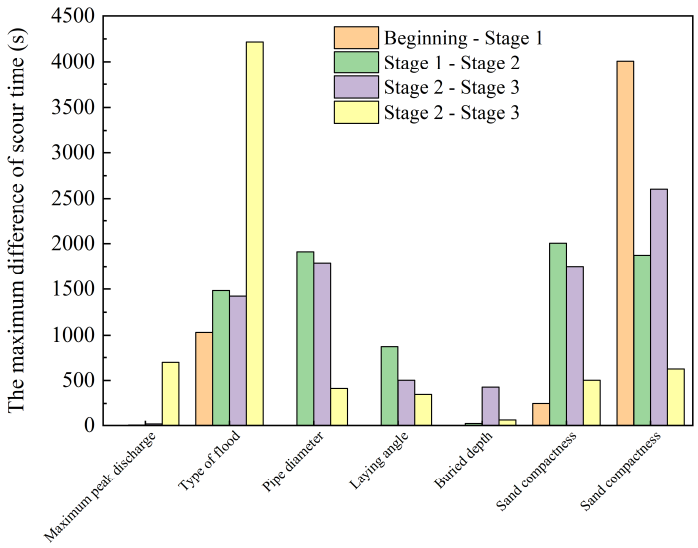


**Figure 16.** The maximum difference of scour time.

After achieving erosion equilibrium, the test section was organized and measured. The remaining measured bed sediment volume was subtracted from the initial bed sediment volume (trapezoidal test sand section, upper bottom 60 cm, lower bottom 80 cm, height 8 cm, width 56.2 cm) to obtain the bed sediment volume carried away by the water flow. The amount of sand erosion in the test section under various test conditions is presented in Figure 17.

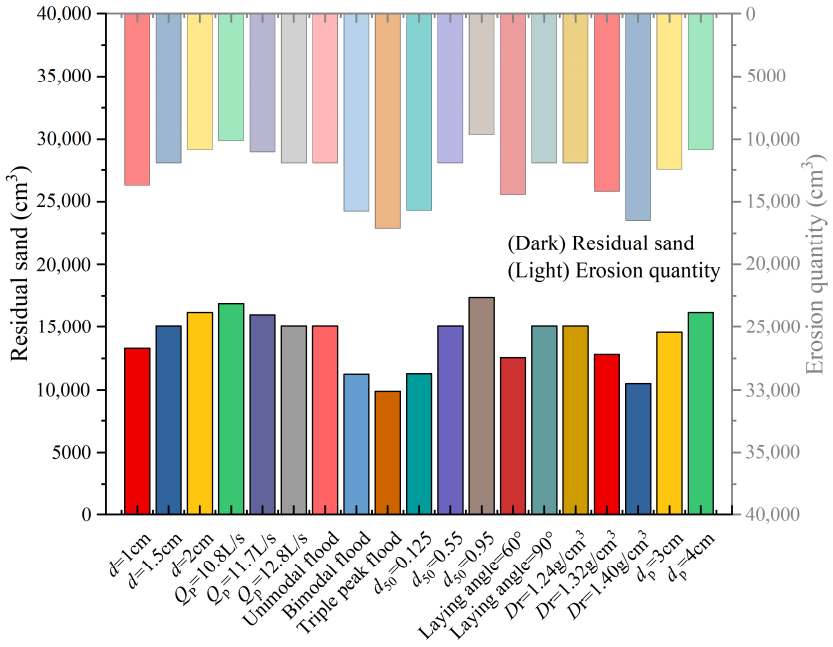


**Figure 17.** Volume statistics of eroded sand in the experimental section.

From Figure 17, it can be observed that the primary influencing factor of sand bed erosion around river bottom crossing pipelines under the action of unsteady flow was the type of flood, with the secondary factor being the relative density. As the number of flood peaks increased, the compactness of the riverbed also increased. However, conversely, the anti-erosion ability of the riverbed around the pipe weakened. When the particle size of the bed sand was larger, resulting in a smaller peak flow rate and a firmer riverbed around the pipeline, the anti-erosion ability was stronger.

## 4. Conclusions

Based on the statistics of accidents in oil and gas pipelines, the suspended instability of pipelines is a crucial cause of pipeline explosions and leakages. Particularly during flood periods, incidents of pipeline suspension are commonplace. For instance, the oil and gas pipeline crossing the Jialing River was exposed due to flood erosion, posing potential safety hazards. To gain insight into the local erosion and suspension process of pipelines under flood action and its influencing factors, an experimental study simulating the evolution process of local scour hanging of river bottom crossing pipelines under unsteady flow was conducted. The key conclusions are as follows:

(1) For river bottom crossing pipelines, the evolution process of the suspended riverbed near the pipeline under unsteady flow action comprises five stages: riverbed cutting, pipeline exposure, micro-pore formation, pipeline suspension, and scour balance. Furthermore, during the local erosion process of underwater crossing pipelines, eddy currents cause the incision of the riverbed. Once the pipeline is exposed, the combined effect of eddy currents and seepage-induced micro-pores at the pipeline's base lead to local erosion. Under unsteady flow conditions, the process of local scour and suspension of pipelines is different compared to constant flow. The erosion pit expansion stage is absent, and the scour duration is shorter. This suggests that pipelines are more prone to suspension during flood periods.

(2) After achieving scouring equilibrium, the maximum scouring range and depth of the scouring hole around the pipeline were precisely measured. Based on erosion data collected under identical conditions, the maximum difference was determined. It was discovered that the maximum peak discharge was the primary influencing factor for the maximum range and depth of the scouring pit. As the maximum peak discharge increases, as well as the Froude number. A higher Froude number indicates a faster

water flow, resulting in a greater maximum scouring depth at the pipeline's base and a reduced scour time required to achieve scouring equilibrium.

(3) The volume of sand carried away by water flow was obtained by calculating the remaining volume of sand in the test section. As the number of flood peaks increased, the anti-erosion ability of the riverbed around the pipeline gradually weakened. However, as the particle size of the bed sand increased, the anti-erosion ability of the riverbed strengthened. It is recommended to choose a protective layer with larger particles when laying pipelines near rivers. This helps to prevent erosion of the riverbed around the pipeline. After flooding, it is important to conduct timely maintenance of pipelines to guarantee their reliability and functionality.

(4) The water flow conditions referred to in this article are from the measured flood results of three hydrological stations in the southwestern mountainous areas of China. However, the flood conditions in mountainous areas are completely different from those in plains, so the research conclusions of this article are only applicable to the conditions of flood erosion in mountainous areas.

(5) This paper primarily focused on analyzing the local erosion and suspension evolution process of the sandy riverbed surrounding pipelines. However, the slope protection section in this experiment should be expanded in length and the inclination should be slowed down in future research to simulate the riverbed more realistically. In addition, the impact of secondary flow on the erosion process should be given more attention. In the case of low flow velocity, secondary flow may have a significant impact on the erosion of riverbed sand. Future studies will continue to explore these aspects in greater detail.

**Author Contributions:** Data curation, Y.X.; Writing—original draft, C.F.; Writing—review & editing, T.Z. All authors have read and agreed to the published version of the manuscript.

**Funding:** This research was funded by Chongqing Water Conservancy Science and Technology Project grant number CQSLK-2023003, the National Natural Science Foundation of China grant number 52109149 and 52279095, the basic science and advanced technology research projects of Chongqing Science and Technology Committee grant number cstc2021jcyj-msxmX0155, Special Key Program for Technological Innovation and Application Development in Chongqing grant number CSTB2022TIAD-KPX0198, Chongqing Water Conservancy Science and Technology Project grant number CQSLK-2022001, Major Science and Technology Program of the Ministry of Water Resources grant number SKS-2022076.

**Data Availability Statement:** The data presented in this study are available on request from the corresponding author. The data are not publicly available due to the ownership of the data by the affiliated institution.

**Acknowledgments:** The following projects are thanked for their financial support during this research: 1. Chongqing Water Conservancy Science and Technology Project. 2. The National Natural Science Foundation of China. 3. The basic science and advanced technology research projects of Chongqing Science and Technology Committee. 4. Special Key Program for Technological Innovation and Application Development in Chongqing. 5. Chongqing Water Conservancy Science and Technology Project. 6. Major Science and Technology Program of the Ministry of Water Resources.

**Conflicts of Interest:** The authors declare no conflict of interest.

## References

1. Bing, H. Analysis of large excavation crossing schemes for large and medium-sized rivers. *China Petrochem.* **2016**, 151. [CrossRef]
2. Wen, B. Prevention and control of debris flow disasters in oil and gas pipelines. *Ind. Saf. Environ. Prot.* **2008**, *34*, 27–29. [CrossRef]
3. Zhang, J.Y.; Du, J.S. Accident analysis of pipeline fracture caused by flood. *Oil Gas Storage Transp.* **2000**, 16–19. [CrossRef]
4. Zhang, Z.M.; Chiew, Y.M.; Ji, C.N. Experimental study on local scour around a forced vibrating pipeline in unidirectional flows. *Coast. Eng.* **2022**, *176*, 104162. [CrossRef]
5. Hu, R.; Wang, X.; Liu, H.; Leng, H.; Lu, Y. Scour Characteristics and Equilibrium Scour Depth Prediction around a Submarine Piggyback Pipeline. *J. Mar. Sci. Eng.* **2022**, *10*, 350. [CrossRef]

6. Postacchini, M.; Brocchini, M. Scour depth under pipelines placed on weakly cohesive soils. *Appl. Ocean Res.* **2015**, *52*, 73–79. [CrossRef]
7. Gao, F.-P.; Han, X.-T.; Cao, J.; Sha, Y.; Cui, J.-S. Submarine pipeline lateral instability on a sloping sandy seabed. *Ocean Eng.* **2012**, *50*, 44–52. [CrossRef]
8. Zhao, E.; Shi, B.; Qu, K.; Dong, W.; Zhang, J. Experimental and Numerical Investigation of Local Scour Around Submarine Piggyback Pipeline Under Steady Current. *J. Ocean Univ. China* **2018**, *17*, 244–256. [CrossRef]
9. Cheng, Y.Z.; Lu, X.H.; Yi, L.; Hu, Y.C.; Li, X.C. Sorting of sand grains around submarine pipelines under the oblique wave. *Adv. Water Sci.* **2016**, *27*, 735–742. [CrossRef]
10. Cui, F.; Du, Y.; Hao, X.; Peng, S.; Bao, Z.; Peng, S. Experimental Study on Local Scour and Related Mechanical Effects at River-Crossing Underwater Oil and Gas Pipelines. *Adv. Civ. Eng.* **2021**, *2021*, 6689212. [CrossRef]
11. Damroudi, M.; Esmaili, K.; Rajaie, S.H. Effect of Pipeline External Geometry on Local Scour and Self-Burial Time Scales in Current. *J. Appl. Fluid Mech.* **2021**, *14*, 103–115. [CrossRef]
12. Sumer, B.M.; Hatipoglu, F.; Fredsøe, J. Wave scour around a pile in sand, medium dense, and dense silt. *J. Waterw. Port Coast. Ocean. Eng.* **2007**, *133*, 14–27. [CrossRef]
13. Dogan, M.; Arisoy, Y. Scour regime effects on the time scale of wave scour below submerged pipes. *Ocean Eng.* **2015**, *104*, 673–679. [CrossRef]
14. Hairsine, P.; Sander, G.; Rose, C.; Parlange, J.-Y.; Hogarth, W.; Lisle, I.; Rouhipour, H. Unsteady soil erosion due to rainfall impact: A model of sediment sorting on the hillslope. *J. Hydrol.* **1999**, *220*, 115–128. [CrossRef]
15. Pontillo, M.; Schmocker, L.; Greco, M.; Hager, W.H. 1D numerical evaluation of dike erosion due to overtopping. *J. Hydraul. Res.* **2010**, *48*, 573–582. [CrossRef]
16. Hong, S.; Biering, C.; Sturm, T.W.; Yoon, K.S.; Gonzalez-Castro, J.A. Effect of Submergence and Apron Length on Spillway Scour: Case Study. *Water* **2015**, *7*, 5378–5395. [CrossRef]
17. Evangelista, S. Experiments and Numerical Simulations of Dike Erosion due to a Wave Impact. *Water* **2015**, *7*, 5831–5848. [CrossRef]
18. Wang, Z.K.; van der Heijdent, G.H.M.; Tang, Y.G. Localised upheaval buckling of buried subsea pipelines. *Mar. Struct.* **2018**, *60*, 165–185. [CrossRef]
19. Wang, Z.K.; Duan, N.; Soares, C.G. Controlled lateral buckling of subsea pipelines triggered by imposed residual initial imperfections. *Ocean Eng.* **2021**, *233*, 109124. [CrossRef]
20. Yang, Q.; Sun, M.; He, M.; Yang, Q. Evolution features of riverbeds near underwater crossing line pipes: An experimental study. *China Acad. J. Electron. Publ. House* **2019**, *39*, 110–117. [CrossRef]
21. Wu, Y.; Chiew, Y.-M. Mechanics of Pipeline Scour Propagation in the Spanwise Direction. *J. Waterw. Port Coast. Ocean Eng.* **2015**, *141*, 04014045. [CrossRef]
22. Haipei, Z.; Wei, Z.; Weifeng, W. Numerical analysis of local scour modal monitoring of underwater pipeline structure. *Yellow River* **2020**, *42*, 134–135+137.
23. Liu, M.-M. Numerical investigation of local scour around submerged pipeline in shoaling conditions. *Ocean Eng.* **2021**, *234*, 109258. [CrossRef]
24. Sharafati, A.; Yasa, R.; Azamathulla, H.M. Assessment of Stochastic Approaches in Prediction of Wave-Induced Pipeline Scour Depth. *J. Pipeline Syst. Eng. Pract.* **2018**, *9*, 04018024. [CrossRef]
25. MacVicar, B.; Chapuis, M.; Buckrell, E.; Roy, A. Assessing the Performance of In-Stream Restoration Projects Using Radio Frequency Identification (RFID) Transponders. *Water* **2015**, *7*, 5566–5591. [CrossRef]
26. Williams, R.D.; Measures, R.; Hicks, D.M.; Brasington, J. Assessment of a numerical model to reproduce event-scale erosion and deposition distributions in a braided river. *Water Resour. Res.* **2016**, *52*, 6621–6642. [CrossRef]
27. Dysarz, T.; Szałkiewicz, E.; Wicher-Dysarz, J. Long-Term Impact of Sediment Deposition and Erosion on Water Surface Profiles in the Ner River. *Water* **2017**, *9*, 168. [CrossRef]
28. Eshev, S.; Gaimnazarov, I.; Latipov, S.; Mamatov, N.; Sobirov, F.; Rayimova, I. The beginning of the movement of bottom sediments in an unsteady flow. *E3S Web Conf.* **2021**, *263*, 02042. [CrossRef]
29. Zhao, T.; Ma, T.; Fu, C.; Zhang, C. Experimental Study on Wide-Graded Soil Transport in Unsteady Flow. *Processes* **2023**, *11*, 1965. [CrossRef]
30. Lin, S.Y.; Miao, R.; Yi, L.Q. Hydrological features of rivers in southwest China. *J. Mt. Sci.* **1999**, *17*, 240–243. [CrossRef]